analytical chemistry

Article

pubs.acs.org/ac

Chemical Two-Photon Fluorescence

Guillermo Carrone and Roberto Etchenique*

Departamento de Química Inorgánica, Analítica y Química Física, INQUIMAE, Facultad de Ciencias Exactas y Naturales, Universidad de Buenos Aires, Ciudad Universitaria Pabellón 2 AR1428EHA Buenos Aires, Argentina

Supporting Information

ABSTRACT: We describe a method based on a caged fluorescent molecule that can act as a chemical two-photon probe. It is composed of an organic fluorophore and a ruthenium−bipyridine complex that acts as a photoremovable quencher. For the fluorophore to be emissive, two independent photons must act on the molecule: the first photon frees the fluorescent ligand from the Ru complex and the second photon excites the fluorescence. In this two-photon regime, the emission is not proportional to the excitation intensity but rather to its second power, as in traditional two-photon systems based on ultrashort pulsed high-power lasers. This quadratic relationship implies a much higher spatial precision on the *z*-axis when the probe is used in a microscopy technique. The chemical nature of the two-photon excitation mechanism allows the use of inexpensive low-power lasers.

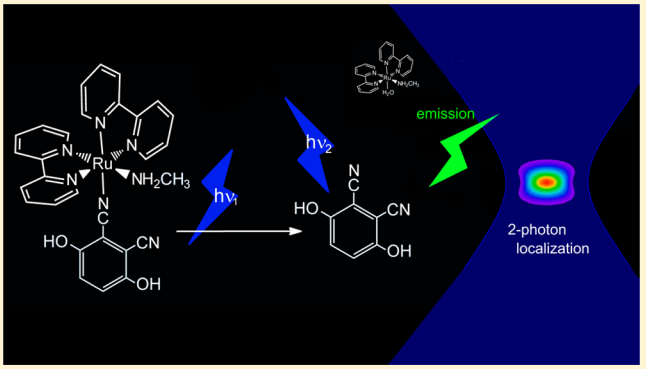

Fluorescence spectroscopy is a very widespread technique in analytical chemistry. Its uses a range of materials, from macrocomponents to traces and from single measurements to high-throughput imaging. It has been used to detect and quantify inorganic species, organic molecules, biological entities of many types, and also to develop very powerful techniques as confocal and high-resolution microscopy.

In usual fluorescence techniques, the emission intensity is linearly related to the excitation power (I_0). This relationship holds, especially at low concentrations, when the absorbance of the sample is proportional to the fraction of absorbed light, $(I_0 - I)/I_0$.

With the advent of lasers—and, thus, very high power focused light—the phenomenon of two-photon absorption and molecular emission was detected in solids[1] and in solution.[2] When the light intensity is high enough, two photons of low energy (long wavelength) can be absorbed the same as if they were one photon of twice the frequency. The result is the population of an excited state from which fluorescence or phosphorescence emission can occur. This effect was used in very early works to monitor carbon monoxide concentration in a flame.[3]

The revolution in combining fluorescence imaging with two-photon excitation came some years later, when Denk reported the first two-photon scanning fluorescence microscope and showed that the quadratic relationship between excitation and emission intensities, characteristic of two-photon absorption, led to a very high spatial resolution.[4] From this seminal work and, mainly, due to their exquisite *z*-axis resolution, microscopy techniques based on two-photon absorption have flourished in many fields of the sciences, mainly in imaging[5−7] and uncaging techniques.[8−11]

The main drawback of two-photon fluorescence techniques is the extremely high instantaneous power needed to excite the sample. Simplifying, the two photons required to reach the excited state must arrive within a very short period of time, on the order of femtoseconds, to allow their simultaneous absorption. This fact implies very high instantaneous light power and, thus, ultrashort pulses to keep the average intensity low enough to prevent photodamage. To achieve both needs, the use of femtosecond pulsed lasers such as Ti-sapphire oscillators (which are voluminous and very expensive) is mandatory.

The only alternative to this strategy was given by Augustine,[12] who used a double-caged approach in order to obtain a two-photon chemical uncaging of glutamate in neural tissue. Since two independent reactions—and, therefore, two photons—are needed to release the neurotransmitter glutamate from its caged form, the concentration of glutamate in a given point is not proportional to the light intensity but to its second power exactly as in optical two-photon excitation. The "chemical-2P advantage" consists of the fact that the two photons must arrive within the diffusional time, much longer than electronic transition times, and very low power lasers can be used. On the other hand, visible or ultraviolet (UV) light, instead of infrared (IR), must be used, with the subsequent lower penetration being due to a higher Tyndall scattering.

Received: January 11, 2015
Accepted: March 18, 2015
Published: March 18, 2015

DOI: 10.1021/acs.analchem.5b00131
Anal. Chem. 2015, 87, 4363−4369

In this paper, we present an approach to circumvent the use of femtosecond lasers for two-photon imaging through a mechanism analogous to that of Augustine et al.: chemical two-photon fluorescence. In this approach, our probe will not fluoresce until two independent photons respectively activate and excite its emission. The activation process consists of the photouncaging of a fluorescent ligand from the coordination sphere of a Ru complex, which acts as a quencher. In this way, the emission intensity will be proportional to the square of the excitation intensity. We show that this quadratic response implies an enhanced spatial resolution, in the same way that is obtained using traditional two-photon techniques but using inexpensive laser modules at instantaneous intensities that are up to 9 orders of magnitude lower.

EXPERIMENTAL SECTION

All reagents but one were commercially available and used as received: $Ru(bpy)_2Cl_2$ was synthesized according to the literature.[13] UV-vis spectra were obtained using a Ocean Optics CHEM2000 diode-array spectrometer. NMR spectra were obtained using a 500 MHz Bruker AM-500. HESI mass spectrometry was performed using a Thermo Scientific Q-Exactive with a Orbitrap detector. All syntheses were performed by degassing the solutions with argon prior to heating, to prevent oxidation of the ruthenium aqua complexes. The photorelease quantum yields were measured by irradiating the samples with calibrated solid-state 405-nm laser diodes. Irradiation inside NMR tubes was done by using an array of 10 high-power light-emitting diodes (LEDs) (525 nm, 25 nm full width at half maximum (fwhm)). A fluorescence quantum yield of DCHQ (ϕ_f = 0.33) was measured using a calibrated laser diode (405-nm excitation), and a solution of Coumarine 6 in ethanol (ϕ_f = 0.78) was used as a standard. Fluorescence lifetimes were measured using a pulsed laser diode (445 nm, 300 ps), a Becker and Hickl Model SPC 130 acquisition board, and a Model MPD 50 avalanche diode. All the measurements were done at 25 °C.

Syntheses. *$[Ru(bpy)_2(CH_3NH_2)Cl]PF_6$.* A total amount of 894 mg of $Ru(bpy)_2Cl_2$ (1.72 mmol) was dissolved in 40 mL of ethanol and stirred 60 min. The formation of the $[Ru(bpy)_2Cl(H_2O)]^+$ complex was determined by its absorption band at 490 nm. After formation of the aqua complex, 140 mg of CH_3NH_2.HCl (2.09 mmol) was dissolved in 1.92 mL of NaOH (1 M) and was added and left under stirring during 120 min. The solution was precipitated with an excess of KPF_6 0.5 M. Yield = 49%. ^{1}H NMR (D_2O): δ 1.92 (t, 3H, J = 6.6 Hz), 3.60 (m, 1H, J = 6.3 Hz), 3.75 (m, 1H, J = 6.3 Hz), 7.05 (t, 1H, J = 6.8 Hz), 7.14 (t, 1H, J = 6.6 Hz), 7.61 (d, 1H, J = 5.5 Hz), 7.72 (t, 1H, J = 8.2 Hz), 7.75 (d, 1H, J = 5.9 Hz), 7.82 (t, 1H, J = 8.6 Hz), 7.81 (t, 1H, J = 7.5 Hz), 7.83 (t, 1H, J = 7.4 Hz), 7.84 (t, 1H, J = 6.6 Hz), 8.20 (t, 2H, J = 7.8 Hz), 8.31 (d, 1H, J = 8.2 Hz), 8.37 (d, 1H, J = 8.2 Hz), 8.54 (d, 1H, J = 7.1 Hz), 8.55 (d, 1H, J = 7.1 Hz), 9.23 (d, 2H, J = 5.5 Hz).

$[Ru(bpy)_2(CH_3NH_2)(DCHQ)]Cl_2$. Forty milligrams (40 mg) of $[Ru(bpy)_2(CH_3NH_2)Cl]PF_6$ (64 μmol) was dissolved in 300 μL of acetone and 5 mL of water, and 1 g of DOWEX-Cl anionic resin was added and left under stirring for 20 min. The solution was evaporated at reduced pressure until a volume of 2 mL was attained. Thirty milligrams (30 mg) of dicyanohyroquinone (DCHQ, 188 μmol) was disolved in 1 mL of water that had been previously degassed with argon, and 250 μL of 1 M NaOH was added. The following procedures were done under illumination from deep red light, to avoid photolysis of the complex. The DQCH solution was added and heated at 50 °C in a sealed tube for 72 h. Two hundred microliters (200 μL) of HCl (1 M) was added to precipitate the DCHQ in excess, centrifuged, and the remaining solution was precipitated with 0.1 M $NaBPh_4$. The yellow complex $[Ru(bpy)_2(MeNH_2)(DCHQ)](BPh_4)_2$ was separated by centrifugation, washed with five portions of distilled water and dissolved in 500 μL of acetone, to be precipitated with an excess of 3 M LiCl in methanol. Yield 18%.

^{1}H NMR (D_2O): δ 2.08 (t, 3H, J = 6.4 Hz), 3.57 (m, 1H), 3.90 (m, 1H), 7.12 (s, 2H), 7.17 (t, 1H, J = 6.7 Hz), 7.25 (t, 1H, J = 6.7 Hz), 7.63 (d, 1H, J = 5.2 Hz), 7.80 (d, 1H, J = 5.7 Hz), 7.82 (t, 1H, J = 7.1 Hz), 7.85 (t, 1H, J = 7.1 Hz), 7.87 (t, 1H, J = 8.0 Hz), 7.94 (t, 1H, J = 7.7 Hz), 8.23 (t, 1H, J = 7.8 Hz), 8.25 (t, 1H, J = 7.9 Hz), 8.34 (d, 1H, J = 8.1 Hz), 8.42 (d, 1H, J = 8.1 Hz), 8.55 (d, 1H, J = 7.7 Hz), 8.57 (d, 1H, J = 8.0 Hz), 9.10 (d, 1H, J = 5.4 Hz), 9.50 (d, 1H, J = 5.7 Hz).

$[Ru(bpy)_2(MeNH_2)(VACN)](PF_6)_2$. Thirty two milligrams (32 mg) of $[Ru(bpy)_2(MeNH_2)Cl]PF_6$ (51 μmol) was dissolved in 300 μL of acetone, and 2 mL of water containing 0.5 g of DOWEX-Cl exchange ion resin were added. It was stirred during 15 min, the resin was filtered off and the solution heated at 60 °C for 1 h. After formation of the aqua complex, 4 μL of a VACN (48 μmol) was added. The solution was heated at 50 °C in a sealed tube during 4 h, cooled to 0 °C and precipitated with KPF_6. Yield: 63%. ^{1}H NMR (acetone-d^6): δ 2.19 (t, 3H, J = 6.8 Hz), 3.72 (m, 2H), 3.96 (m, 1H), 4.20 (m, 1H), 4,98 (dt, 1H, J = 17 Hz, 1.9 Hz), 5.13 (dt, 1H, J = 10 Hz, 1.7 Hz), 5.74 (m, 1H), 7.40 (t, 1H, J = 7.2 Hz), 7.42 (t, 1H, J = 7.2 Hz), 7.82 (d, 1H, J = 5.7 Hz), 7.95 (t, 1H, J = 6.8 Hz), 7.99 (d, 1H, J = 5.8 Hz), 8.02 (t, 1H, J = 7.2 Hz), 8.04 (t, 1H, J = 8.0 Hz), 8.06 (t, 1H, J = 8.0 Hz), 8.37 (t, 1H, J = 7.9 Hz), 8.41 (t, 1H, J = 7.8 Hz), 8.65 (d, 1H, J = 6.9 Hz), 8.67 (d, 1H, J = 6.9 Hz), 8.82 (d, H, J = 8.3 Hz), 8.83 (d, 1H, J = 8.3 Hz), 9.46 (d, 1H, J = 4.9 Hz), 9.64 (d, 1H, J = 4.9 Hz).

RESULTS AND DISCUSSION

Figure 1 shows the absorption and emission spectra of dicyanohydroquinone (DCHQ) in aqueous solutions at pH 3, 7, and 11. The changes are due to the different protonation states of the diphenol molecule.[14]

Figure 2 shows the absorption of the complex $[Ru(bpy)_2(CH_3NH_2)(DCHQ)]^{n+}$ at the same three pH values (pH 3, 7, and 11).

When solutions of $[Ru(bpy)_2(CH_3NH_2)(DCHQ)]^{n+}$ are irradiated with visible light in the range of its Ru-bpy MLCT transition, the complex behaves as most complexes of its family,[15] releasing the less-donor ligand DCHQ. Figure 3 shows the ^{1}H NMR spectra of a $[Ru(bpy)_2(CH_3NH_2)(DCHQ)]Cl_2$ solution in D_2O during *in situ* irradiation on the NMR tube using a high-power green (525 nm) LED array. Upon irradiation, the only photoproducts are the ligand DCHQ (showing its typical singlet at 7.22 ppm) and the aqua complex $[Ru(bpy)_2(CH_3NH_2)(H_2O)]^{2+}$.

The reaction can be quantitatively followed through UV-vis absorption or emission. Figure 4 shows the photolysis process using a 405-nm laser diode at pH 3, pH 7 (top), and pH 11 (bottom).

Given the power of the irradiation beam, its optical path, the volume, and concentration of the complex solution, it is possible to calculate the differential amount of product as

DOI: 10.1021/acs.analchem.5b00131
Anal. Chem. 2015, 87, 4363−4369

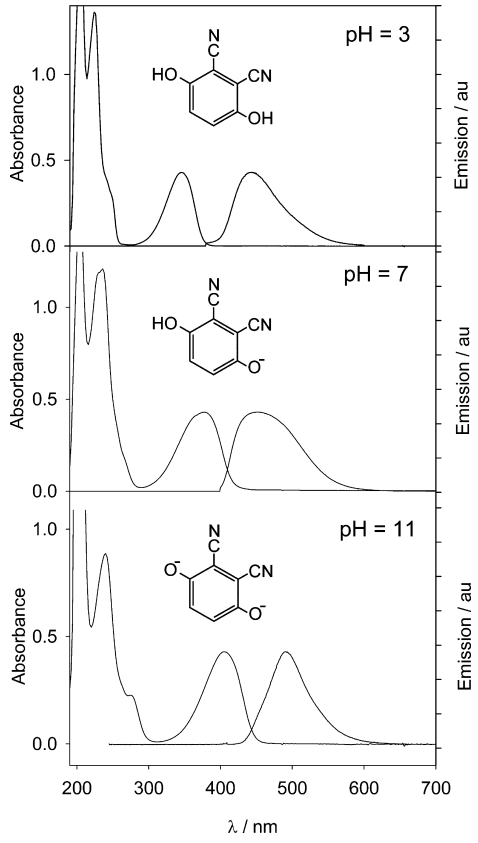

Figure 1. Absorption and emission spectra of dicyanohydroquinone at different pH in aqueous solution: (top) HCl solution at pH 3, λ_{exc} = 360 nm; (middle) NaH_2PO_4/Na_2HPO_4 buffer at pH 7, λ_{exc} = 405 nm; and (bottom) NaOH solution at pH 11, λ_{exc} = 405 nm.

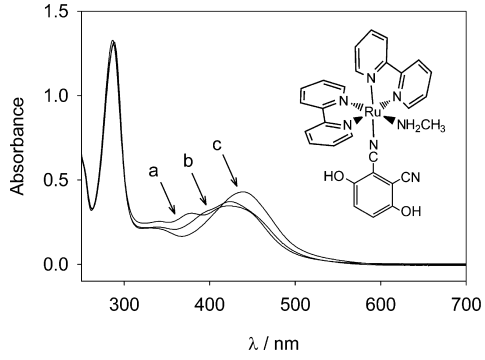

Figure 2. Absorption spectra of the complex $[Ru(bpy)_2(CH_3NH_2)(DCHQ)]Cl_2$ at different pH in aqueous solution. From left to right: pH 3 (plot a), pH 7 (plot b), and pH 11 (plot c). The depicted structure corresponds to pH 3.

$$\frac{dn_P}{dt} = I_{beam}(1 - 10^{-Abs_T})\frac{Abs_R}{Abs_T}\varphi_{PC} \quad (1)$$

where n_P are the number of moles of product, I_{beam} is the intensity of the incident light (in Einsteins/s), Abs_T and Abs_R are the total solution's absorbance and the reactant's absorbance, respectively, and φ_{PC} is the quantum yield of photolysis. The irradiation intensity was measured using a calibrated photodiode. The value of φ_{PC} is the adjustable parameter and was obtained by integrating eq 1 with a finite differences algorithm.[11]

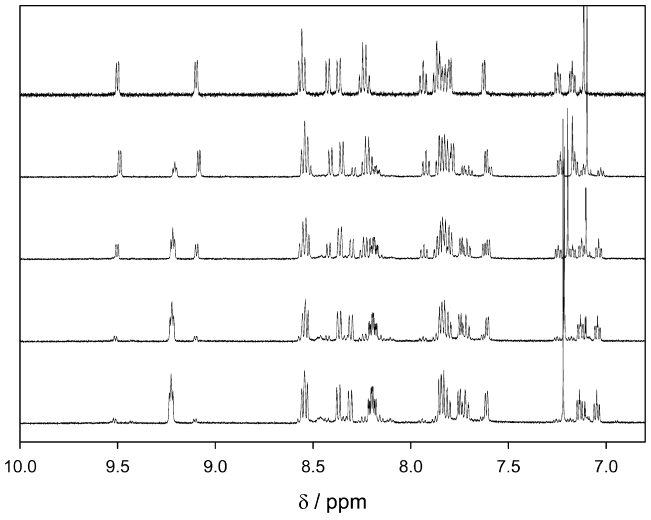

Figure 3. ^1H NMR aromatic signals of a solution of $[Ru(bpy)_2(CH_3NH_2)(DCHQ)]Cl_2$ in D_2O during photolysis inside an NMR tube (from top to bottom). The irradiation was performed with a set of 525-nm green LEDs. The singlet at 7.22 ppm after irradiation corresponds to the photodelivery of the DCHQ ligand.

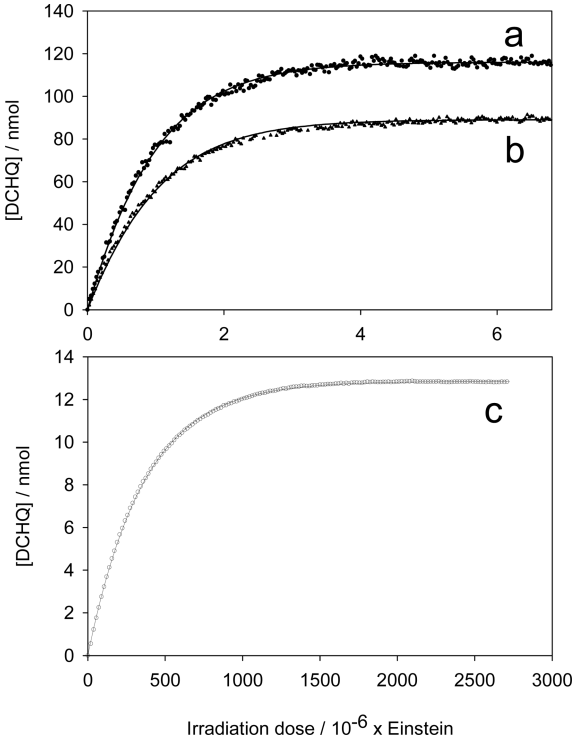

Figure 4. Photolysis of aqueous solutions of $[Ru(bpy)_2(CH_3NH_2)(DCHQ)]Cl_2$ during irradiation at 405 nm at (a) pH 7 (c = 58 μM, I_L = 4.17 mW), (b) pH 3 (c = 45 μM, I_L = 4.55 mW), and (c) pH 11 (c = 9.1 μM, I_L = 127 mW). Note the different scales of plot c, which implies less-efficient photodelivery(by 3 orders of magnitude). Photolysis plots a and b were measured through absorbance changes, while plot c was obtained using emission spectroscopy.

The quantum yield of DCHQ release decreases abruptly with pH, being ~1000 times lower at pH 11 than at acidic or neutral pH (see Table 1). This behavior can be explained by the negative charge of DCHQ at high pH, which electrostatically prevents the photorelease by recapture of the ligand by the highly positive charged Ru center.

DOI: 10.1021/acs.analchem.5b00131
Anal. Chem. 2015, 87, 4363−4369

Table 1. Quantum Yields of Photolysis of the Nitrile Ligand at 450 nm for the Complex $[Ru(bpy)_2(CH_3NH_2)(DCHQ)]^{n+}$ and Its Analogue $[Ru(bpy)_2(CH_3NH_2)(VACN)]^{2+}$

	pH = 3	pH = 7	pH = 11
$[Ru(bpy)_2(CH_3NH_2)(DCHQ)]^{n+}$	0.114 ± 0.018	0.133 ± 0.022	$(2.2 \pm 0.2) \times 10^{-4}$
$[Ru(bpy)_2(CH_3NH_2)(VACN)]^{2+}$	0.248 ± 0.007	0.248 ± 0.005	0.251 ± 0.008

In order to test this suggestion, the photolysis process of the analogous complex $[Ru(bpy)_2(CH_3NH_2)(VACN)]^{2+}$ (VACN = allyl cyanide) was also measured. Its structure is depicted in the Supporting Information. The transition energy in Ru-bpy complexes is strongly dependent on the donor ability of the coordinated group[15] but is barely dependent on the rest of the ligand structure. Therefore, any coordinated nitrile would be useful for this comparison. VACN is an advantageous choice, because its water solubility is similar to DCHQ, but benzonitrile and acetonitrile yielded similar results. In this complex, the coordination is also achieved through a nitrile group but no deprotonation of the ligand is possible. As expected, the quantum yield of photolysis remains high at any pH. In this complex, the absorption of the ligand is not present, and all the photons are indeed absorbed through the Ru-bpy MLCT band;[15] therefore, the photolysis yields are higher than that of the DCHQ complex, as shown in Table 1.

At pH >7, the photolysis of the complex can be followed through fluorescence spectroscopy. Figure 5 shows some

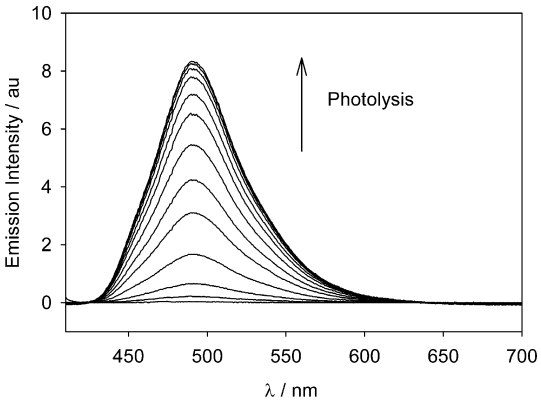

Figure 5. Fluorescence spectra during irradiation of a cuvette containing a 9.1 μM aqueous solution of $[Ru(bpy)_2(CH_3NH_2)(DCHQ)]Cl_2$. Irradiation at 405 nm was performed with a collimated laser diode at 90° of the emission detection path. Total irradiation time = 6500 s. I_L = 127 mW.

selected emission spectra during irradiation at pH 11 that reflects the increasing concentration of the highly emissive DCHQ. The fluorescence increases by ~200 fold during the photolysis. The initial emission (which is very low and appears merged with the *x*-axis in the figure) can be due to a very low intrinsic fluorescence of the complex, some free ligand in the preparation, or an impurity. If any of the last cases were proven to be true, the change in fluorescence between the coordinated and the free DCHQ would be even greater than 200 fold.

Fluorescence lifetime measurements of basic solutions of DCHQ yielded a value of τ = 5.2 ns (see the Supporting Information). Solutions of the complex $[Ru(bpy)_2(CH_3NH_2)(DCHQ)]Cl_2$ did not present emission, but only fluorescence, because of the free ligand, which is a product of its photodelivery. Given that the stationary emission of the complex is ~200-fold lower than that of the free DCHQ, it is expected to have a lifetime of τ < 26 ps, which is below the time limit of our measurement system (this is consistent with an almost-complete deactivation).

The fact that the absorption band of DCHQ after coordination is almost unaltered suggests that the quenching mechanism is energy transfer from the emissive state to the MLCT Ru band. The conjugation of the nitriles with the aromatic ring implies that electron conductivity can be established between the ligand and the metallic center and a high degree of electron wave function overlap can be present, which would allow a Dexter mechanism.[16] Since the distance between the ligand and the Ru center is short, inverse Forster energy transfer is also possible[17−19] Figure 6 shows the

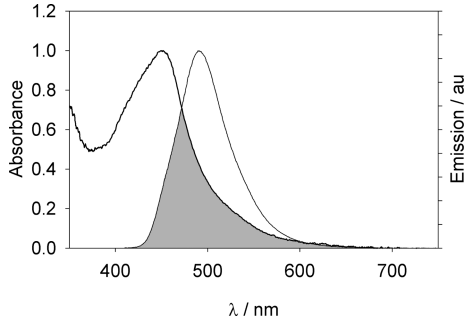

Figure 6. Absorption spectra of $[Ru(bpy)_2(CH_3NH_2)(VACN)]^{2+}$ (left, c = 125 μM in 10 mM NaOH) and normalized fluorescence spectra of DCHQ in 10 mM NaOH solution under 405-nm excitation (right). The gray area shows the overlap between the emission of DCHQ and the absorption of the complex that allows high-efficiency energy transfer, which is responsible for the emission quenching in the complex $[Ru(bpy)_2(CH_3NH_2)(DCHQ)]^{2+}$.

absorption of the complex $[Ru(bpy)_2(CH_3NH_2)(VACN)]^{2+}$, which exhibits its strong MLCT band centered at 452 nm. (This complex shares the same structure with $[Ru(bpy)_2(CH_3NH_2)(DCHQ)]^{n+}$, allowing direct inspection of the MLCT band, which is somewhat obscured in the latter, because of the presence of DCHQ absorption in the same region.) As can be seen, there is an important overlap (gray area) between the emission of DCHQ and the absorption of the complex. This overlap integral $J(\lambda)$ amounts to 2.9×10^{14} M^{-1} cm^{-1} nm^4, which corresponds to a Forster characteristic distance of R_0 = 3.5 nm. Given that the ligand has a much shorter distance than R_0, a near-unity energy trasfer efficiency is expected, in agreement with the observed results.

Given that (i) the local concentration of free DCHQ will be dependent on the light irradiation and (ii) the emission intensity is dependent on both light irradiation and DCHQ concentration, the immediate conclusion is that, for low absorbances and low irradiation power, the fluorescence intensity would scale as the second power of excitation intensity. This relationship holds when the local concentration of free DCHQ is much lower than the concentration of the complex. Figure 7 shows the emission intensity of a solution of $[Ru(bpy)_2(CH_3NH_2)(DCHQ)]^{2+}$ during irradiation with a

DOI: 10.1021/acs.analchem.5b00131
Anal. Chem. 2015, 87, 4363−4369

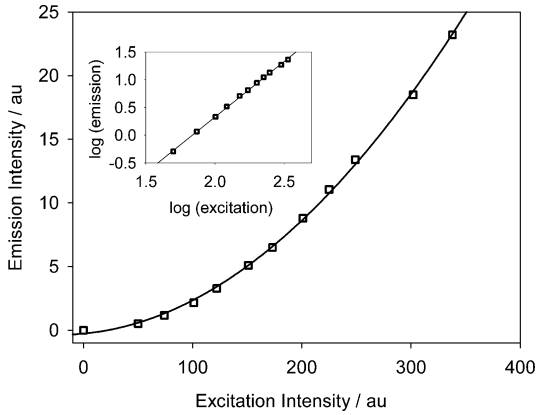

Figure 7. Emission intensity versus excitation intensity in a flow cell. A 100 μM aqueous solution of $[Ru(bpy)_2(CH_3NH_2)(DCHQ)]Cl_2$ was forced into a capillary cell by gravity. (see Figure S8 in the Supporting Information). The fluorescence intensity was measured using an Ocean Optics spectrometer with a 50-μm-diameter fiber optics device focused onto the focal point of the irradiation.

variable laser intensity. The irradiation was performed in a flow cell in order to have a fresh solution at any instant of the experiment. The obtained quadratic response, which is characteristic of a two-photon excitation process, is evident. The log–log plot in Figure 7 (inset) shows a slope of 1.99, in accordance with a two-photon mechanism.

We have briefly tested this complex as a probe for a chemical two-photon microscopy technique. As a preliminary test, a wide 405-nm laser beam was focused through a 20× long-working-distance objective into a fluorescence cuvette under continuous agitation to prevent photobleaching and/or accumulation of photoproducts in the focal zone. A camera placed at a right angle was used to take a picture of the light cone. The procedure was followed using the ligand DCHQ and the complex $[Ru(bpy)_2(CH_3NH_2)(DCHQ)]^{2+}$, both at pH 11. The results are shown in Figure 8. While the free ligand behaves as usual, yielding a bicone of light, because of its linear response emission-excitation, the solutions of the complex show that the emissive zone is confined to the focal vicinity. This is the key characteristic that improves the z-axis resolution in two-photon techniques.

For this chemical two-photon approach to work, two independent photons must respectively activate and excite the fluorophore within the diffusional time.

In order to get the insight of the conditions in which this technique would be feasible, we performed several calculations of the system's behavior by means of a numerical resolution of the differential equations involved in the photolysis–difussion model.

For a Gaussian beam incident normal to the objective (z-axis) in a lateral infinite medium containing a low concentration of the complex, we have

$$\frac{\partial c(x,\,t)}{\partial t} = \nabla(D\nabla c(x,\,t) + \frac{(c_a - c)I_{eff}}{z^2 + \sigma^2}\exp\left(-\frac{r^2}{z^2} + \sigma^2\right) \quad (2)$$

where D is the diffusion coefficient, c_a its analytical concentration of the inactive fluorophore in bulk, c the instantaneous concentration of the active (uncaged) fluorophore at a given time and spatial location, I_{eff} the effective photolysis rate (depending on the light power, the absorption

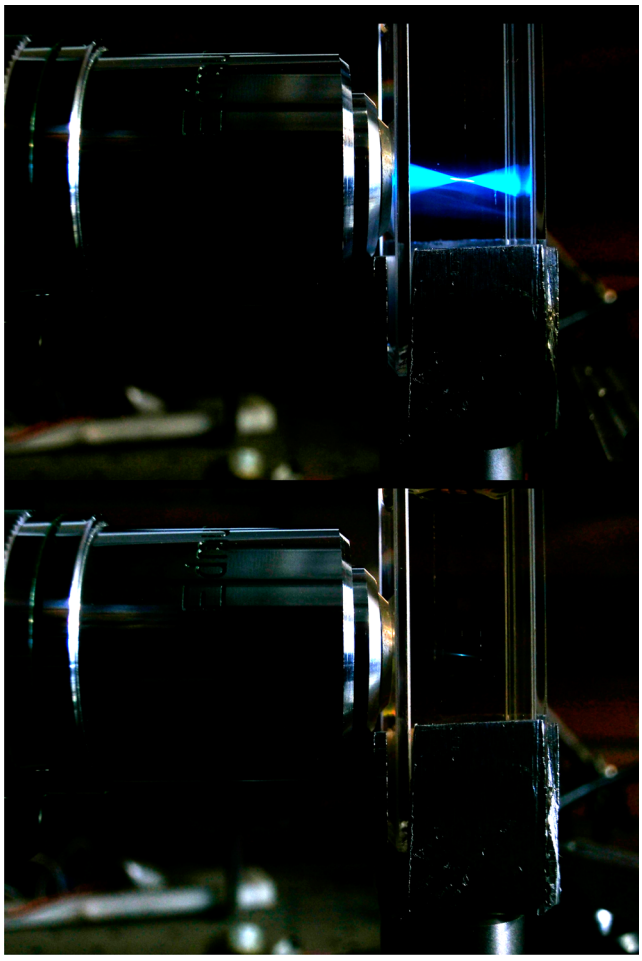

Figure 8. (Top) Focusing of a 405-nm solid-state laser through a 20× objective into a cuvette containing an aqueous solution of DCHQ at pH 12. The emission bicone is characteristic of the one-photon fluorescence. (Bottom) The same laser is focused into a solution of $[Ru(bpy)_2(CH_3NH_2)(DCHQ)]Cl_2$ at pH 11. The impressive two-photon behavior is shown, with the fluorescence being restricted to the focal zone. If the irradiation is continuous, free DCHQ starts to accumulate in neighboring areas and the two-photon effect is lost.

of the complex, and its uncaging quantum yield), z the vertical coordinate, r the radial coordinate (cylindrical symmetry), and σ the minimum radius of the incident beam at focus. At the beginning, $c = 0$ in all space. The differential equations were solved by a numerical procedure using FlexPde 5.0 software. Some simplifications were assumed, as a numerical aperture $N_A = 1$ for the incident beam and the same diffusion coefficient for the inactive (Ru complex) and active (DCHQ) fluorophores. The minimum width of the beam was set to be 1 μm (poorer than diffraction-limited focusing, including any possible distortion at the real optical setup). A typical script is given in the Supporting Information.

Once the irradiation takes place at time $t = 0$, the active fluorophore DCHQ begins to accumulate, as shown in Figure 9. During the first part of the photolysis, the system behaves as a two-photon chemical process, and gradually moves to one-photon characteristics with time. For the parameters used in the simulation, the free fluorophore concentration rises quite linearly until 2 μs, then the curvature of a pseudo-exponential trend becomes important. Ten microseconds (10 μs) after the beginning of the photolysis, the DCHQ concentration at the

DOI: 10.1021/acs.analchem.5b00131
Anal. Chem. 2015, 87, 4363–4369

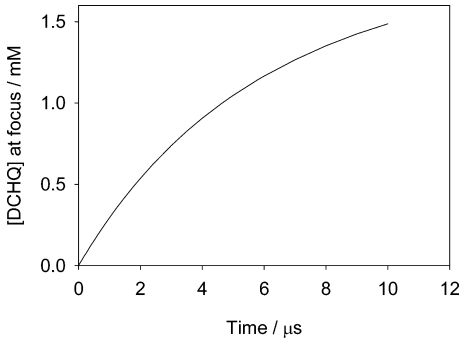

Figure 9. Concentration of free DCHQ at the focal point in function of time during focused irradiation of the complex $[Ru(bpy)_2(CH_3NH_2)(DCHQ)]Cl_2$ in aqueous solution (pH 11). The simulation was done using eq 2 under the conditions described in the main text.

focal point reached ~71% of the bulk complex concentration (c_{bulk} = 2 mM).

Figure 10 shows the comparison plots in three-dimensional (3D) cylindrical coordinate space (r = 0 is the cylinder axis),

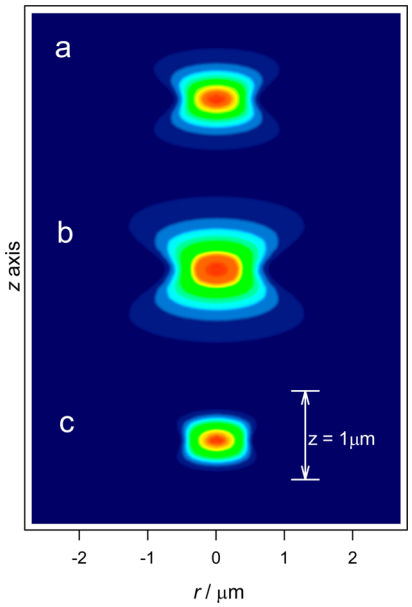

Figure 10. (a) Excitation intensity in 3D cylindrical coordinates of focused light through an N_A = 1 objective. (For a usual fluorophore, this plot would coincide with its emission intensity.) (b) Free DCHQ concentration due to the uncaging of the complex $[Ru(bpy)_2(CH_3NH_2)(DCHQ)]$ at pH 11 and the subsequent diffusion. (c) Overall emission of the system, taking into account the excitation intensity and the free DCHQ concentration profiles, showing the z-axis enhanced focusing of the system. The simulation was done using eq 2 under the conditions described in the main text.

showing the light excitation profile (Figure 10a), the DCHQ concentration (Figure 10b), and the effective emission (Figure 10c) after 10 μs of irradiation time. Note that the localization of the active fluorophore, together with the high light density at the focal point, implies a much-sharper z localization of the emission in the bottom plot, as expected for a two-photon technique.

The space-time dependence of free DCHQ concentration and overall emission can be seen in videos provided in the Supporting Information. The two-photon behavior is even stronger at lower photolysis grades. With the parameters used, at 2 μs, the photolysis conversion is ~26% of the full concentration and, under these conditions, the system behaves almost exactly as a physical two-photon method. Figure 11

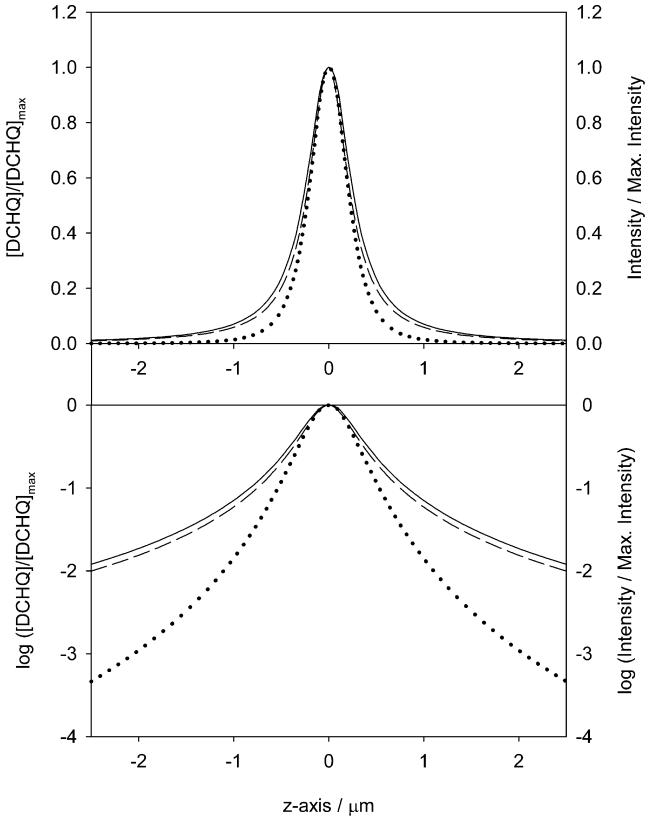

Figure 11. Concentration of DCHQ (full line), excitation intensity (dashed), and overall emission (dotted line), as a function of the distance to the focus through the z-axis. Top plot shows a linear scale; bottom plot shows a logarithmic scale (units relative to maximum light intensity).

shows the light intensity profile, the DCHQ concentration profile, and the subsequent emission on the z-axis in the vicinity of the focal point. The top plot comparison of the overall emission versus the relative excitation intensity shows the much steeper focus in the z-axis. The semilogarithmic plot at the bottom is even more informative to show the change in the z-focusing steepness, as shown experimentally in Figure 8 (bottom).

In a nonlinear two-photon regime, both photons must excite the fluorophore within a very short time (on the order of the absorption transition), which implies an extremely high instantaneous light power. Usual parameters for a 1 W Ti-sapphire laser are t = 100 ps, f = 80 MHz, which implies that an instantaneous power of 125 kW/pulse is needed to excite most two-photon-capable fluorophores. The need of this extremely high power can be diminished by devising new probes with enhanced two-photon cross sections,[20,21] which allow the use of Q-switched Nd:YAG microlasers that have nanosecond pulses at lower repetition rates. While the price of a standard Ti-sapphire laser is in the range of 100 000 USD, a Nd:YAG microlaser costs ~10 000 USD, which is a significant improvement. [USD denotes U.S. dollars.] In the chemical two-photon approach, even considering a freely moving fluorophore, both photons must be harvested within the

DOI: 10.1021/acs.analchem.5b00131
Anal. Chem. 2015, 87, 4363−4369

diffusional time (microseconds), instead of the transition time (femtoseconds). For standard temperatures, this fact implies that the instantaneous power can be reduced to the order of 1 mW, allowing the use of even solid-state laser diodes in pulsed mode (as the used in this work), with typical prices of ∼100 USD. On the other hand, the chemical two-photon strategy uses the same wavelength of the linear regime excitation, instead of the low-energy IR photons of a normal two-photon process. This characteristic implies that the additional advantage of lower scattering in heterogeneous samples is not present in a chemical two-photon process.

Although this system can be regarded as a proof of principle for chemical two-photon microscopy, the present design has two important drawbacks. An ideal chemical two-photon probe should have zero-emissions before uncaging. The residual fluorescence, even being low, acts as a background and, therefore, must be diminished. On the other hand, although, at high pH, the overall photolysis of the complex is very low, eventually all the DCHQ is delivered and the preparation behaves as a usual one-photon fluorescent probe. This problem could be circumvented by means of an auxiliary coordination position that ensures almost-100% recapture after transient photolysis or by using systems that renew the fluorophore in the case of inspecting cavities or microfluidic devices in three dimensions with high *z*-axis resolution. Further research on the probe and related techniques is being done in order to achieve this goal.

CONCLUSIONS

We have devised a new caged fluorophore molecule capable of increasing its fluorescence by more than a 100 times upon irradiation with light of the same wavelength of that excitation. By means of this mechanism, the emission intensity scales with the square of the excitation intensity, becoming a chemical two-photon fluorophore. Similar to traditional two-photon probes, chemical two-photon excitation led to a narrower depth of focus with improved *z*-axis accuracy. On the other hand, instantaneous power can be 10^9 times lower than in classical two-photon excitation. As for classical two-photon absorption processes using appropriate chromophores with optimized two-photon absorption cross sections,[21] inexpensive laser modules operating in the range of 1 mW can replace the femtosecond Ti-sapphire laser. Further design and development of the probes and related optical system, in order to achieve full reversibility and no emission background, are being pursued.

ASSOCIATED CONTENT

Supporting Information

NMR spectra, mass spectroscopy (MS), time-resolved emission measurements, and video files of space-temporal simulation of free fluorophore concentration and emission during focused irradiation are provided as Supporting Information. This material is available free of charge via the Internet at http://pubs.acs.org.

AUTHOR INFORMATION

Corresponding Author

*E-mail: rober@qi.fcen.uba.ar.

Notes

The authors declare no competing financial interest.

ACKNOWLEDGMENTS

This research was supported by the National Agency for Science and Technology Promotion, CONICET, and University of Buenos Aires. R.E. is a member of CONICET.

REFERENCES

(1) Kaiser, W.; Sugano, S.; Wood, D. L. *Phys. Rev. Lett.* **1961**, *6*, 605.
(2) Adelman, A. H.; Verber, C. M. *J. Chem. Phys.* **1963**, *39*, 931−933.
(3) Haumann, J.; Seitzman, J. M.; Hanson, R. K. *Opt. Lett.* **1986**, *11*, 776−778.
(4) Denk, W.; Strickler, J. H.; Webb, W. W. *Science* **1990**, *248*, 73−76.
(5) Nikolenko, V.; Poskanzer, K. E.; Yuste, R. *Nat. Methods* **2007**, *4*, 943−950.
(6) Svoboda, K.; Yasuda, R. *Neuron* **2006**, *50*, 823−839.
(7) Chaigneau, E.; Oheim, M.; Audinat, E.; Charpak, S. *Proc. Natl. Acad. Sci. U.S.A.* **2003**, *100*, 13081−13086.
(8) Judkewitz, B.; Roth, A.; Hausser, M. *Neuron* **2006**, *50*, 180−183.
(9) Donato, L.; Mourot, A.; Davenport, C. M.; Herbivo, C.; Warther, D.; Léonard, J.; Bolze, F.; Nicoud, J.-F.; Kramer, R. H.; Goeldner, M.; Specht, A. *Angew. Chem.* **2012**, *51*, 1840−1843.
(10) Fino, E.; Araya, R.; Peterka, D. S.; Salierno, M.; Etchenique, R.; Yuste, R. *Front. Neural Circuits* **2009**, *3*, 1−9.
(11) Araya, R.; Andino-Pavlovsky, V.; Yuste, R.; Etchenique, R. *ACS Chem. Neurosci.* **2013**, *4*, 1163−1167.
(12) Pettit, D. L.; Wang, S. S.; Gee, K. R.; Augustine, G. J. *Neuron.* **1997**, *19*, 465−471.
(13) Viala, C.; Coudret, C. *Inorg. Chim. Acta* **2006**, *359*, 984−989.
(14) Brown, R. G.; Porter, G. *J. Chem. Soc. Faraday Trans.* **1977**, *73*, 1281−1285.
(15) Pinnick, D. V.; Durham, B. *Inorg. Chem.* **1984**, *23*, 1440−1445.
(16) Inokuti, M.; Hirayama, F. *J. Chem. Phys.* **1965**, *43*, 1978−1989.
(17) Filevich, O.; García-Acosta, B.; Etchenique, R. *Photchem. Photobiol. Sci.* **2012**, *11*, 843−847.
(18) Bahreman, A.; Cuello-Garibo, J. A.; Bonnet. *Dalton Trans.* **2014**, *43*, 4494−4505.
(19) Carrone, G.; Gantov, F.; Slep, L. D.; Etchenique, R. *J. Phys. Chem. A* **2014**, *118*, 10416−10424.
(20) Spangenberg, A.; Malval, J.-P.; Akdas-Kilig, H.; Fillaut, J.-L.; Stehlin, F.; Hobeika, N.; Morlet-Savary, F.; Soppera, O. *Macromolecules* **2012**, *45*, 1262−1269.
(21) Martineau, C.; Lemercier, G.; Andraud, C.; Wang, I.; Bouriau, M.; Baldeck, P. L. *Synth. Met.* **2003**, *138*, 353.

DOI: 10.1021/acs.analchem.5b00131
Anal. Chem. 2015, 87, 4363−4369